

## Supporting Information for

### **10% solar-to-fuel conversion with non-precious materials**

Cassandra R. Cox,<sup>\*, a</sup> Jungwoo Z. Lee,<sup>b</sup> and Daniel G. Nocera,<sup>\*, a</sup> Tonio Buonassisi<sup>b,\*</sup>

<sup>a</sup>*Department of Chemistry and Chemical Biology, Harvard University, Cambridge, Massachusetts 02138, USA.* <sup>b</sup>*Massachusetts Institute of Technology, Cambridge, MA 02139, USA.*

<i>Index</i>	<i>Page</i>
Mini-module fabrication	S2
Product crossover calculation	S3
<b>Table 1.</b> PV characteristics for c-Si mini-modules	S4
<b>Figure S1.</b> Steady-state NiB <sub>1</sub> activity with H <sub>2</sub>	S5
<b>Figure S2.</b> Decay of the open circuit voltage of the PV mini-modules	S6
<b>Figure S3.</b> Specific conductance measurements for electrolyte solutions	S7
<b>Figure S4.</b> $J_{OP}$ for PV-EC device in 1 M KOH	S8
<b>Figure S5.</b> $J$ - $V$ curves of PV mini-modules and catalysts	S9

## Additional Experimental Details

### Mini-module fabrication

Mini-modules were fabricated using commercially available single-junction Czochralski silicon solar cells. Mini-cells were cut out of commercial size wafers by laser scribing with a 1064 nm pulsed laser and mechanical cleaving. Mini-cells were electrically connected via solar tabbing wire and silver epoxy. The mini-module was constructed by sequentially layering glass, EVA, solar cells, and EVA. The glass maintains structural integrity while EVA provides water protection. The mini-module was encapsulated using a double layer vacuum press heated to 120 °C. With the module in the lower chamber of the vacuum press, both the upper and lower chambers were held under vacuum for 5 min. The upper chamber was vented to atmospheric pressure for 5 min to remove air bubbles through the induced pressure difference between the two chambers. The lower chamber was vented and the mini-module was allowed to cool to room temperature. Excess EVA was removed and the mini-module was stored to protect against mechanical and water degradation.

### Estimation of current associated with crossover on SFE

The impact on the SFE due to H<sub>2</sub> oxidation can be estimated by examining the mass-transport limited current density, which is given by:

$$J_L = \frac{nFDc_b}{\delta}$$

where,  $n$  is the number of electrons,  $F$  is Faraday's constant,  $c_b$  is the bulk concentration of species in solution,  $D$  is the diffusion coefficient ( $5.11 \times 10^{-5} \text{ cm}^2 \text{ s}^{-1}$  for H<sub>2</sub> in water), and  $\delta$  is the Nernst diffusion layer thickness. Assuming H<sub>2</sub> saturation in water ( $7.8 \times 10^{-7} \text{ mol cm}^{-3}$ ), and a reasonable value for  $\delta$  given a planar electrode with no artificially imposed convection is around 0.05 cm (1), which gives a  $J_L$  at the anode for H<sub>2</sub> oxidation of 0.15 mA cm<sup>-2</sup>. This implies that for a 10% SFE (or 8.13 mA cm<sup>-2</sup>) the contribution from product crossover would be at most 0.15 mA cm<sup>-2</sup>, giving a SFE of 9.8%. Figure S1 shows that the experimental measurement of H<sub>2</sub> crossover by the NiBi catalyst is less than that predicted from this calculation; no current from H<sub>2</sub> oxidation is observed, speaking to the selectivity of the catalyst.

---

1. Bockris JO, Reddy AKN, and Gamboa-Aldeco ME, (1998) *Modern electrochemistry* (New York: Plenum Press, c1998-c2000).

**Table S1.** PV characteristics for the 3 and 4-cell c-Si mini-modules.

<b>PV module characteristics</b>	<b>4- cell</b>	<b>3-cell</b>
V <sub>oc</sub> (V)	2.46	1.79
I <sub>sc</sub> (mA)	51.0	52.2
Active Area (cm <sup>2</sup> )	6.0	4.5
Fill Factor	76.9	76.2
Efficiency (%)	16.0	15.8

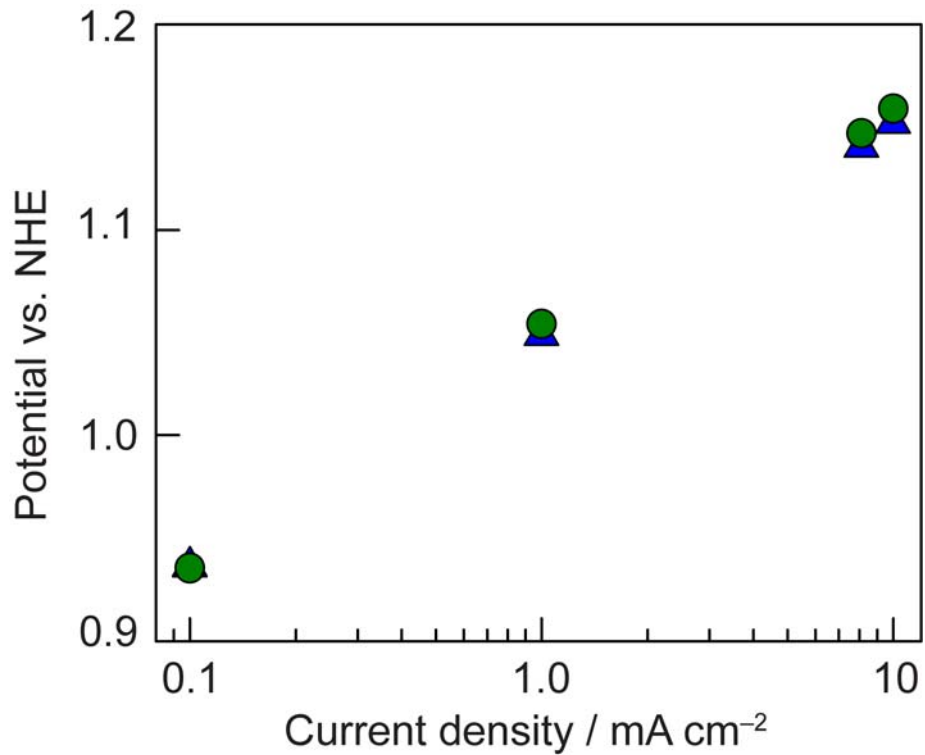


**Figure S1.** Steady-state current voltage behavior for the NiBi operating in 0.5 M KBi /0.5 M K<sub>2</sub>SO<sub>4</sub> pH 9.2 in H<sub>2</sub> saturated solution (green circles) and in Ar saturated solution (blue triangles). The voltage required to achieve a given current density under both conditions is nearly identical, indicating that the contribution of H<sub>2</sub> oxidation at the anode is negligible.

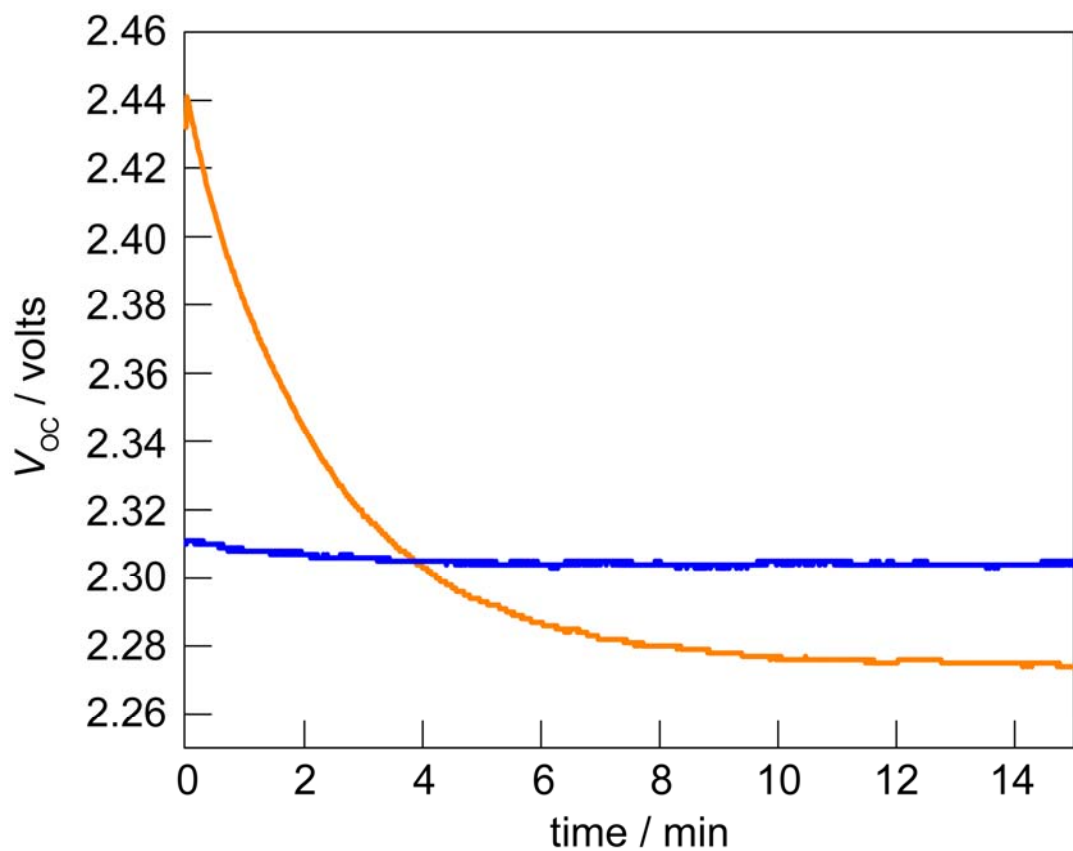


**Figure S2.** Decay of the open circuit voltage of the 4-cell PV mini-module over the course of  $\sim 1$  h. The initial  $V_{OC}$  starts at 2.42 V and decays to a steady-state of 2.27 V after the first 10 min (orange line), which contributes to the initial decline in SFE of the coupled PV-EC device. After overnight illumination the  $V_{OC}$  was measured (blue line) and shows a recovery to 2.31 V, which corresponds to the initial increase in SFE of the PV-EC device during the first 24 h.

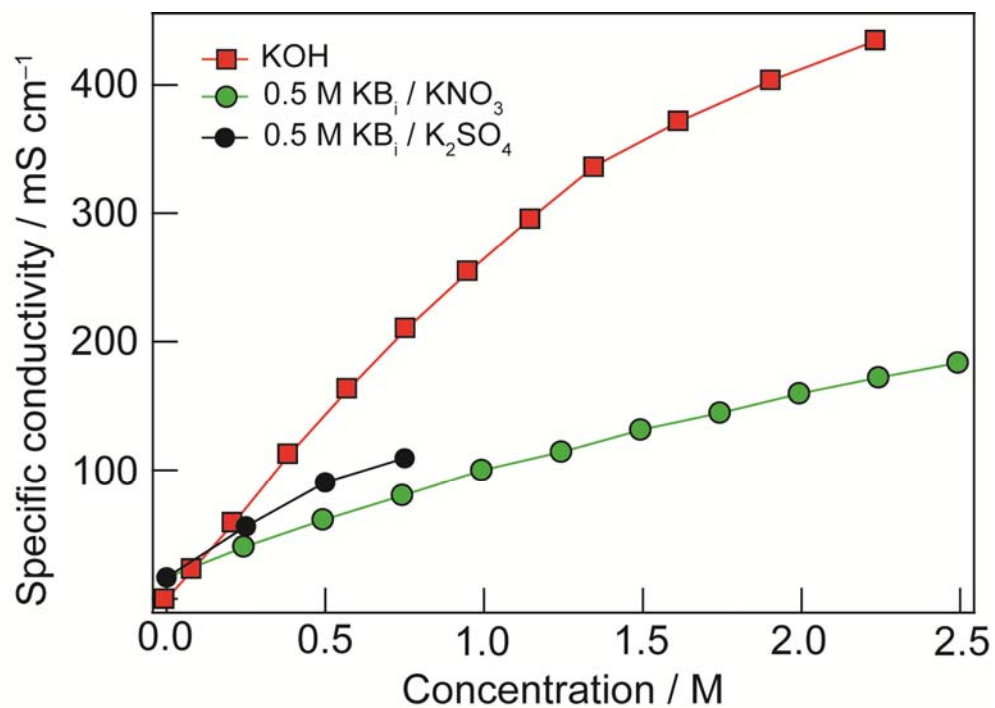


**Figure S3.** Specific conductance measurements for the various electrolytes considered to minimize  $R_{\text{SOL}}$ . KOH is the most conductive electrolyte; in order to operate in pH near neutral regimes 0.5 M KB<sub>i</sub> was used with additional supporting electrolyte.

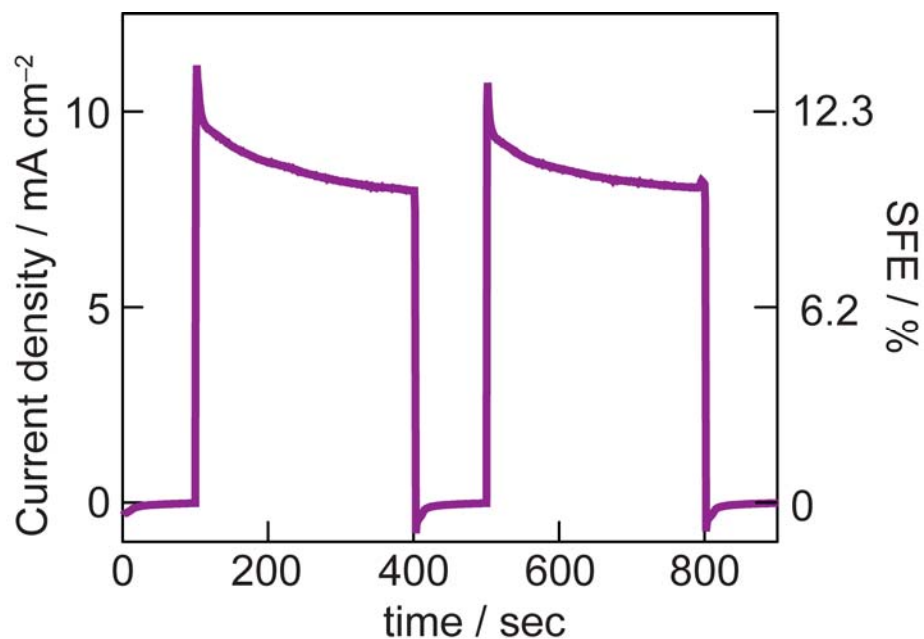


**Figure S4.** Current under chopped illumination representing  $J_{OP}$  for the PV-EC device composed of a 3-cell PV-module, a NiB<sub>i</sub> anode and NiMoZn cathode operating in 1 M KOH (pH 14). Because KOH is a conductive electrolyte, a 12% SFE can be obtained with a 3-cell mini-module as opposed to a 4-cell module. The initial drop in SFE is due to the decrease in PV efficiency, due to heating of the PV module. The chopped illumination illustrates the recovery in SFE.

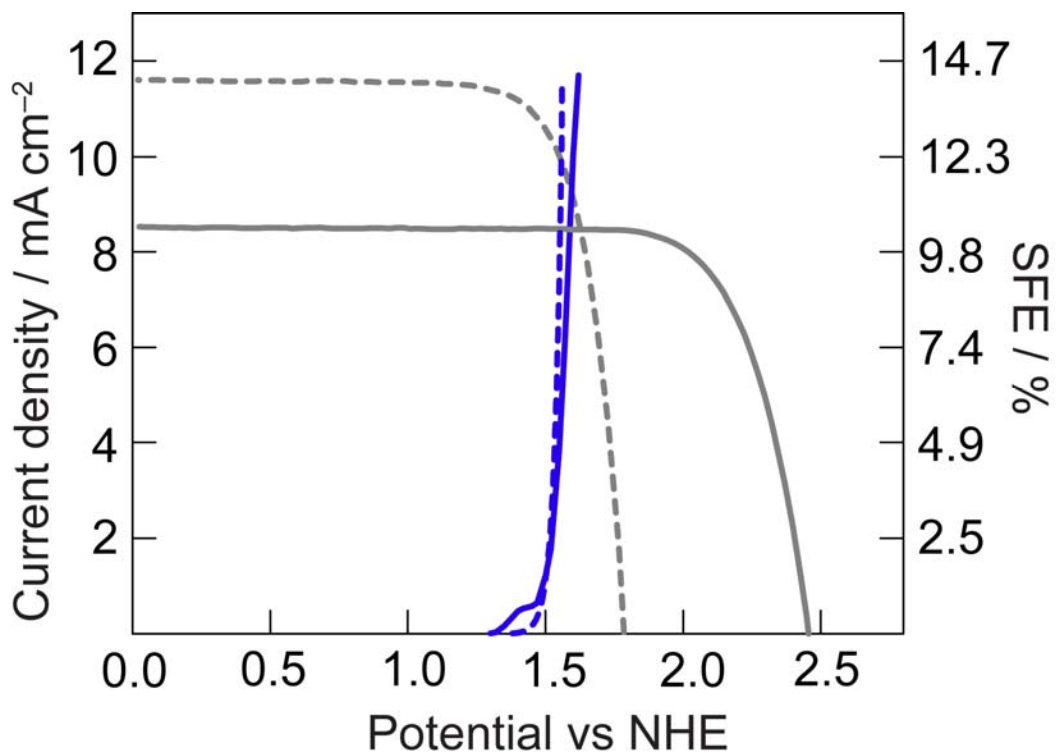


**Figure S5.** *J-V* curves of the individually measured 3 (grey dashed) and 4 (grey solid) cell PV mini-modules and EC curve measured in 1 M KOH. The blue dashed curve shows the ideal *J-V* curve obtained for NiBi and NiMoZn catalysts based on previously reported Tafel analysis and the solid blue curve is the experimentally measured EC curve.